OXFORD

International Journal of Neuropsychopharmacology (2021) 24(2): 142–157

doi:10.1093/ijnp/pyaa075
Advance Access Publication: September 25, 2020
Regular Research Article

REGULAR RESEARCH ARTICLE

Anti-Amnesic and Neuroprotective Effects of Fluoroethylnormemantine in a Pharmacological Mouse Model of Alzheimer's Disease

Simon Couly,Morgane Denus, Mélanie Bouchet, Gilles Rubinstenn, Tangui Maurice

MMDN, Univ Montpellier, INSERM, EPHE, Montpellier, France (Dr Couly, Ms Denus, Ms Bouchet, and Dr Maurice); ReST Therapeutics, Paris, France (Dr Rubinstenn).

Correspondence: Dr T. Maurice, PhD, INSERM UMR_S1198, Université de Montpellier, cc 105, Place Eugène Bataillon, 34095 Montpellier cedex 5, France (tangui.maurice@umontpellier.fr).

ABSTRACT

Background: Current therapies in Alzheimer's disease (AD), including Memantine, have proven to be only symptomatic but not curative or disease modifying. Fluoroethylnormemantine (FENM) is a structural analogue of Memantine, functionalized with a fluorine group that allowed its use as a positron emission tomography tracer. We here analyzed FENM neuroprotective potential in a pharmacological model of AD compared with Memantine.
Methods: Swiss mice were treated intracerebroventricularly with aggregated $A\beta_{25–35}$ peptide and examined after 1 week in a battery of memory tests (spontaneous alternation, passive avoidance, object recognition, place learning in the water-maze, topographic memory in the Hamlet). Toxicity induced in the mouse hippocampus or cortex was analyzed biochemically or morphologically.
Results: Both Memantine and FENM showed symptomatic anti-amnesic effects in $A\beta_{25-35}$-treated mice. Interestingly, FENM was not amnesic when tested alone at 10 mg/kg, contrarily to Memantine. Drugs injected once per day prevented $A\beta_{25-35}$-induced memory deficits, oxidative stress (lipid peroxidation, cytochrome c release), inflammation (interleukin-6, tumor necrosis factor-α increases; glial fibrillary acidic protein and Iba1 immunoreactivity in the hippocampus and cortex), and apoptosis and cell loss (Bcl-2–associated X/B-cell lymphoma 2 ratio; cell loss in the hippocampus CA1 area). However, FENM effects were more robust than observed with Memantine, with significant attenuations vs the $A\beta_{25-35}$-treated group.
Conclusions: FENM therefore appeared as a potent neuroprotective drug in an AD model, with a superior efficacy compared with Memantine and an absence of direct amnesic effect at higher doses. These results open the possibility to use the compound at more relevant dosages than those actually proposed in Memantine treatment for AD.

Key Words: Fluoroethylnormemantine, Alzheimer's disease, symptomatic effect, neuroprotection, Aβ25_35

Introduction

Alzheimer's disease (AD) is characterized by the progressive deterioration of memory, cognition, and autonomy (Bondi et al., 2017). AD is estimated to represent 60%–80% of dementia cases and, at present, there are 50 million AD patients worldwide with its incidence doubling every 5 years after the age of 65 (Brookmeyer et al., 1998). The main clinical manifestations are cognitive dysfunction, memory loss, and changes in personality. The pathology is characterized by the extracellular

Received: July 22, 2020; **Revised:** September 15, 2020; **Accepted:** September 24, 2020

accumulation of aggregating amyloid-β (Aβ) proteins forming senile plaques, intracellular neurofibrillary tangles composed of abnormally phosphorylated tau protein, and a massive neuroinflammation (Selkoe, 1991, 2004; Bondi et al., 2017). Several hypotheses have been proposed to explain AD pathogenesis, thereby involving amyloid cascade (Selkoe, 1991), tau hyperphosphorylation (Frost et al., 2009), neuroinflammation, and oxidative stress (Butterfield and Halliwell, 2019). Toxicity results in synapse loss affecting cholinergic neurons innervating brain structures like the hippocampus or neocortex and seems to be directly responsible for the memory impairments. Synapse loss results from the failure of neurons to maintain functional dendrites (Bloom, 2014; Avila et al., 2017) and is related to perturbed synaptic Ca^{2+} handling in response to over-activation of glutamate receptors, namely N-methyl-D-aspartate receptors (NMDARs) (Mota et al., 2014). Therefore, although the underlying causes and ideal strategy for a curative treatment remain elusive, present treatments are based on acetylcholinesterase inhibitors to maintain the cholinergic tonus and on a NMDAR antagonist, 3,5-Dimethyl-tricyclo[3.3.1.13,7]decyl amine (Memantine) (Danysz and Parsons, 2003; Wang and Reddy, 2017; Floch et al., 2018). Memantine is prescribed in moderate-to-severe AD, and combining acetylcholinesterase inhibitors and Memantine led to higher benefits on cognitive alterations in patients (Patel and Grossberg, 2011; Deardorff and Grossberg, 2016). Memantine acts as a noncompetitive NMDAR antagonist with moderate affinity, being an open NMDAR channel blocker with fast off-rate, but it also shows a preferential blockade of extrasynaptic NMDARs (Hardingham and Bading, 2010; Xia et al., 2010; Floch et al., 2018).

Present AD drugs provide only symptomatic benefits in patients (Salomone et al., 2012). In preclinical research models, Memantine, at 20 mg/kg/d, prevented quinolinic acid-induced lesion–induced learning impairments in rats in the T maze and radial arm maze tests (Misztal et al., 1996; Zajaczkowski et al., 1996; Lang et al., 2004). Memantine at 5 mg/kg/d was also effective in rats against the $A\beta_{1-40}$ + ibotenic acid-induced memory deficits (Nakamura et al., 2006). Using intraventricularly injected lipopolysaccharide, a model of AD-like neuroinflammation, learning deficits in the water-maze test were prevented by Memantine at 10 mg/kg (Rosi et al., 2006). Finally, in mice receiving intraventricular injection of oligomerized $A\beta_{25-35}$, Memantine attenuated learning deficits at 1 mg/kg (Maurice, 2016). In transgenic mouse models of AD, Memantine at 30 mg/kg/d for 3 weeks improved acquisition in the water maze in APP/PS1 mice (Minkeviciene et al., 2004) and at 30 mg/kg for 12 weeks improved animals learning abilities and decreased memory loss in $APP_{Swe}/PS1^{dE9}$ mice fed with high-fat diet (Ettcheto et al., 2018). At 2 mg/kg/d, it alleviated retention deficits in the water-maze to the level of wild-type controls (Van Dam et al., 2005). Memantine is therefore neuroprotective in preclinical rodent models of AD. The reason why this effect does not translate in patients remains to be understood, but it is worth noting that the proposed Memantine (Ebixa) AD treatment is 20 mg/d, which corresponds to a lower dose than those used in preclinical neuroprotection studies. Recent results indicated that Memantine levels in the cerebrospinal fluid during memantine treatment are not sufficient to trigger NMDA response (Valis et al., 2019).

Memantine and several derivatives have been fluorinated and tested as radiotracers of positron emission tomography (PET) for the in vivo labeling of NMDARs (Ametamey et al., 2002). Among them, [^{18}F]-Fluoromethylmemantine and [^{18}F]-Fluoroethylnormemantine ([^{18}F]-FENM) showed promising in vitro and in vivo binding in mice and monkeys, with good brain accumulation (Samnick et al., 1998; Ametamey et al., 1999; Salabert et al., 2015, 2018). [^{18}F]-FENM distribution did not, however, reflect regional NMDAR concentration, owing to high nonspecific uptake in white matter (Ametamey et al., 1999). Although having a moderate affinity (Ki = 3.5 10^{-6} M), the drug showed a good lipohily (logD = 1.93) and [^{18}F]-FENM showed staining colocalization with NMDARs, with highest intensities found in the cortex and cerebellum and lowest in white matter (Salabert et al., 2015). A low nonspecific binding was also observed when phencyclidine sites were blocked with (R,S)-ketamine (Salabert et al., 2015). As observed for Memantine, FENM is poorly metabolized in vivo with good stability in plasma and plasma protein binding but with a low effective dosimetric dose compared with other PET radiotracers (Salabert et al., 2018).

In the present study, we analyzed the symptomatic and neuroprotective activities of FENM compared with Memantine in the pharmacological model of AD induced by intraventricular injection of $A\beta_{25-35}$ peptide in mice (Maurice et al., 1996). After $A\beta_{25-35}$ injection, mice rapidly develop neuroinflammation, oxidative stress, apoptosis, and learning deficits reminiscent of AD toxicity (Meunier et al., 2006; Villard et al., 2011; Rodriguez Cruz et al., 2017; Maurice et al., 2019). Memantine and FENM were administered in the 0.1- to 10-mg/kg dose range either 7 days after $A\beta_{25-35}$ to examine the symptomatic effects of the drugs or o.d. during 1 week after the $A\beta_{25-35}$ injection to examine their neuroprotective effects (Meunier et al., 2006; Maurice et al., 2019). Learning deficits were analyzed using a battery of behavioral tests, and neuroprotection was also examined in the hippocampus or cortex postmortem using biochemical analyses of neuroinflammation, oxidative stress, and apoptosis markers as well as immunohistochemical and histological analyses of the mouse brains.

MATERIALS AND METHODS

Animals

Male Swiss CD-1 (RjOrl:SWISS) mice or C57Bl/6j mice were from Janvier (Le Genest Saint Isle, France). All experiments were done with Swiss mice except the Hamlet test, which used C57Bl/6j mice. Mice were aged 7–9 weeks and housed in groups of 8–10 mice, with free access to food and water, in a regulated environment (23°C ± 1°C, 40%–60% humidity, 12-hour-light/-dark cycle. Animal procedures were conducted in adherence with the European Union Directive 2010/63 and the ARRIVE guidelines (Kilkenny et al., 2010) and authorized by the National Ethic Committee (Paris, France).

Drugs and Peptides

Memantine was from Sigma-Aldrich (Saint Quentin-Fallavier, France). FENM was from M2i Life Sciences (Saint Cloud, France). Drugs were solubilized in physiological saline (NaCl 0.9%, vehicle solution) in a stock solution (2 mg/mL corresponding to the dose of 10 mg/kg) and dilutions done from this stock solution. The stock solutions were stored at +4°C up to 2 weeks. Drugs were administered i.p. in a volume of 100 µL per 20 g body weight.

The amyloid-β[25–35] peptide ($A\beta_{25-35}$) was from Eurogentec (Angers, France). It was solubilized in distilled water at 3 mg/mL and stored at –20°C until use. Before injection, the peptide was incubated at 37°C for 4 days, allowing oligomerization (Pike et al., 1993). Control injection was performed with vehicle solution (distilled water) as we previously described no effect of antisense or control peptide, and intracerebroventricularly (ICV) injections were done as described (Maurice et al., 1996).

Experimental Series

We examined 2 effects of the drugs. First, symptomatic effects were analyzed in $A\beta_{25-35}$-treated mice by injecting the drugs just before the behavioral tests. Second, the neuroprotection was analyzed by repeatedly o.d. injecting the mice for 1 week starting on the day of peptide injection. For symptomatic effects, drugs were injected only on day 8 after $A\beta_{25-35}$ injection, 30 minutes before the behavioral tests: spontaneous alternation, passive avoidance training, session 2 of the object recognition test or each water-maze training sessions (supplementary Figure 1a). A group was tested for spontaneous alternation, passive avoidance, and object recognition in series. As Memantine, and expectedly FENM, has a short half-life in mice (<2 hours; Beconi et al., 2011), all the drug was excreted overnight. A separate group was trained in the Hamlet before $A\beta_{25-35}$ injection to assess topographic memory (supplementary Figure 1b). For neuroprotective effects, drugs were injected o.d. from day 1 to day 7 after $A\beta_{25-35}$ injection (supplementary Figure 1c), and mice were tested for spontaneous alternation, passive avoidance, and object recognition in series. They were killed at day 13 for immunochemistry (group A). A group of mice performed place learning in the water-maze, then were killed at day 16 and used for biochemical assays (group B). An additional series (group C) included mice killed at day 5 after $A\beta_{25-35}$ peptide injection and daily drug injections for assessing cytokine levels by enzyme-linked immunosorbent assays (ELISA).

Behavioral Testing

Procedures for each test are detailed in the supplementary Material and followed our previously published work (Crouzier et al., 2018; Maurice et al., 1996, 2019; Meunier et al., 2006, 2013; Rodriguez Cruz et al., 2017; Villard et al., 2009, 2011). Spontaneous alternation in the Y-maze was used to assess spatial working memory. Long-term nonspatial memory was measured using a step-through passive avoidance test. Recognition memory was analyzed using a novel object test. Spatial reference memory was assessed using place learning in the water-maze. Topographic memory was assessed using the Hamlet test.

Lipid Peroxidation Measures

Mice from group B were killed by decapitation 15 days after $A\beta_{25-35}$ injection, brains were rapidly removed, and the hippocampus dissected out, weighed, frozen in liquid nitrogen, and stored at –80°C until assayed. The level of lipid peroxidation was determined using the modified xylenol oxidation method as previously described (Meunier et al., 2006; Rodriguez Cruz et al., 2017).

Cytochrome C Release

Mice were killed at indicated days after injections and the hippocampus rapidly dissected on ice and kept at –80°C until use. For cytochrome c release experiments, the hippocampus was homogenized with a motorized homogenizer in ice-cold homogenization buffer (250 µM sucrose, 10 mM HEPES, pH 7.4), including a protease and phosphatase inhibitor cocktail (Roche Diagnostics, Meylan, France) in a final volume of 250 µL. Homogenates were centrifuged at 600 *g* for 5 minutes and the supernatant collected and centrifuged again at 10 300 *g* for 20 minutes. The supernatant, corresponding to the cytosolic fraction (C), and the pellet, corresponding to the crude mitochondrial fraction (M), were separated. The mitochondrial fraction was resuspended in 50 µL of ice-cold isolation buffer (250 mM mannitol, 5 mM HEPES, 0.5 mM EGTA, pH 7.4). Protein concentration was determined using a bicinchoninic acid assay (Pierce Biotechnology, Rockford, IL) according to the manufacturer's instructions.

Proteins, 20 µg per lane, were resolved on a 12% SDS-polyacrylamid gel and transferred to a polyvinylidene fluoride membrane (GE Healthcare, Orsay, France). After 1 hour blocking in 5% nonfat dry milk in a 20 mM Tris-buffered saline pH 7.5 buffer containing 0.1% Tween-20, membranes were incubated overnight at 4°C with the following primary antibodies: mouse anti-cytochrome c (dilution 1/1000; BioLegend, San Diego, CA), mouse anti-oxphos-complex IV subunit I (1/1000; Invitrogen Life Technologies, St Aubin, France). After brief washes, membranes were incubated for 1 hour at room temperature with corresponding secondary antibody: goat anti-mouse IgG peroxidase conjugate (1/2000; Sigma-Aldrich). The immunoreactive bands were visualized with the enhanced chemiluminescence reagent (Millipore, Molsheim, France) using an Odyssey Fc fluorescent imaging system (Li-Cor, Eurobio, Courtaboeuf, France). The intensity of peroxidase activity was quantified using the Odyssey Fc software (Li-Cor).

ELISA

Protein contents in tumor necrosis factor-α, interleukin-6 (IL-6), allograft inflammatory factor-1 (Iba-1), glial fibrillary acidic protein (GFAP), B-cell lymphoma 2 (Bcl-2), and Bcl-2–associated X (Bax) were analyzed by ELISA (see Table 1 for kit references). For n = 6–8 animals, both hippocampi were used. The tissue was homogenized after thawing in 1 mL of fresh lysis buffer (3 IS007, Cloud-Clone) and sonicated on ice for 2 × 10 seconds. After centrifugation (10 000 *g*, 5 minutes, 4°C), supernatants were then aliquoted and stocked at –80°C and used within 1 month for ELISA according to the manufacturer's instructions. For each assay, absorbance was read at 450 nm and sample concentration was calculated using the standard curve. Results are expressed in ng of marker per mg of protein and in % of the control (V + V) value.

Brain Fixation and Slicing

At day 13, 5–6 mice from each condition of group A were anesthetized with 200 µL IP of a premix of ketamine (80 mg/kg) and xylazine (10 mg/kg) and transcardially perfused with 50 mL of saline solution followed by 50 mL of Antigenfix (Diapath). The samples were kept for 48 hours post fixation in Antigenfix solution at +4°C. Brains were immersed in a sucrose 30% phosphate buffer saline solution and sliced within 1 month.

Each brain was sliced in an area including the cortex, the nucleus basalis magnocellularis, and the hippocampal formation, between Bregma +1.80 to –2.80 according to Paxinos and Franklin (2004). Serial coronal frozen sections (25 µm thickness) were cut with a freezing microtome (Microm HM 450, Thermo

Table 1. Commercial ELISA Kits Used in the Study

Marker	Supplier	Reference	Batch no.
TNFα	Cloud-Clone Corp	SEA133MU	2F9E677166
IL-6	Cloud-Clone Corp	SEA079MU	72431BCFFC
Iba-1 (AIF1)	Cloud-Clone Corp	SEC288MU	405293E2FE
GFAP	Cloud-Clone Corp	SEA068MU	0F5E05AE12
Bax	Cloud-Clone Corp	SEB343MU	4FBE513B6F
Bcl-2	Cloud-Clone Corp	SEA778MU	089D7E6339

Abbreviations: Bax, bcl-2-like protein 4; Bcl-2, B-cell lymphoma 2, ELISA, enzyme-linked immune-sorbent assay; GFAP, glial fibrillary acidic protein; Iba-1 (AIF1), Allograft inflammatory factor 1; IL-6, interleukin-6; TNFa, tumor necrosis factor-a.

Fisher), collected in a 24-well plate, and stored in cryoprotectant at –20°C. Slices were placed on glass slides, each containing 3 coronal sections from 1 mouse.

Quantification of Viable Neurons in CA1 Using Cresyl Violet Staining

Sections were stained with 0.2% cresyl violet reagent (Sigma-Aldrich), then dehydrated with graded ethanol, treated with xylene, and mounted with Mountex medium (BDH Laboratory Supplies). After mounting, slides were kept drying at room temperature for 24 hours. Examination of the CA1 area was performed using digitalized slices using a Nanozoomer virtual microscopy system (Hamamatsu, Massy, France). CA1 thickness measure and pyramidal cells count were processed using a 20× objective with the cell count macro of ImageJ v1.46 software (NIH). Data were expressed as mean number of viable cells per mm^2 from 4–6 hippocampi for each mouse according to the previously reported method (Villard et al., 2009; Rodriguez Cruz et al., 2017; Maurice et al., 2019).

Immunohistochemical Labeling of Microglia (Iba-1) and Astrocytes (GFAP)

For immunohistochemical labeling, slices in 24-well plates were incubated overnight at +4°C with Rabbit polyclonal anti-Iba-1 (1:250, 019-19 741, Wako) and mouse monoclonal anti-GFAP (1:400, G3893, Sigma-Aldrich). Then, slices were incubated 1 hour at room temperature with secondary anti-rabbit Cy3 (1:1000) and secondary anti-mouse 488 (1:1000) antibodies. Slices were incubated 5 minutes with DAPI 10 µg/mL and rinsed with phosphate buffer saline. Finally, slices were mounted with ProLong (ThermoFischer). Pictures of each slices were taken with a confocal Microscope (Leica SPE).

Statistical Analyses

Analyses were done using Prism v5.0 (GraphPad Software, San Diego, CA). Data were analyzed using 1-way ANOVA (*F* value) followed by a Dunnett's test. Passive avoidance latencies, expressed as median and interquartile range and represented as box-and-whiskers, were analyzed using a nonparametric Kruskal-Wallis ANOVA (*H* value) and post hoc comparisons done using a Dunn's test. Probe test data in the water-maze were presented as time spent in the T and o quadrants. Object preferences were calculated from the number or duration of contacts with the 2 objects. They were analyzed using a 1-sample t test vs the chance level (15 seconds or 50%, respectively). Significance levels were $P<.05$, $P<.01$, and $P<.001$. Statistical data are indicated in the figure legends.

RESULTS

Anti-Amnesic Effects of Memantine and FENM in $A\beta_{25-35}$-Injected Mice

We first analyzed the symptomatic effects of FENM compared with Memantine on $A\beta_{25-35}$-induced learning deficits in mice. Drugs were injected 30 minutes before the tests, particularly before the training session(s) in long-term memory tests, and 7 days after $A\beta_{25-35}$ injection (supplementary Figure 1a). Memantine dose-dependently attenuated $A\beta_{25-35}$-induced spontaneous alternation deficits in mice in a bell-shaped manner (Figure 1a), with a significant effect at 0.3 mg/kg. FENM showed a similar dose-response effect (Figure 1b), and significant attenuation was observed in the 0.3- to 10-mg/kg dose range. In the passive avoidance test, Memantine dose-dependently attenuated $A\beta_{25-35}$-induced deficit in a bell-shaped manner with a significant effect at 0.3 mg/kg (Figure 1c). FENM showed a similar dose-response effect with significance in the 0.1- to 1-mg/kg dose range (Figure 1d). In the object recognition test, drugs were injected before session 2. Drugs did not affect the equal exploration of the 2 similar objects (Figure 1e–f). In session 3, Memantine and FENM attenuated significantly but in a bell-shaped manner the $A\beta_{25-35}$-induced novel object exploration deficit at doses of 0.3 mg/kg and higher (Figure 1g–h).

In the water-maze test, $A\beta_{25-35}$ injection resulted in a moderate attenuation of the decrease in swimming latency to find the platform compared with Veh-treated animals during trials 4 and 5 (Figure 2a), indicating that $A\beta_{25-35}$ fails to affect procedural memory but rather impaired integration of spatial cues that contributed the mouse efficiency to locate the platform in late training sessions. $A\beta_{25-35}$ injection resulted in memory deficits since the time spent in the T quadrant during the probe test was at the random level (15 seconds) contrarily to control animals (Figure 2c). FENM, tested at the most active dose identified previously, 0.3 mg/kg, restored an acquisition profile similar to controls (Figure 2b) and a significantly increased exploration of the T quadrant during the probe test (Figure 2c).

The drug symptomatic effect was finally tested in an alert sign of AD, the spatio-temporal disorientation, as it could be analyzed in the Hamlet test (Crouzier et al., 2018). Mice were trained in the Hamlet for 4 h/d for 2 weeks (supplementary Figure 1b) and identified the maze topography (localization of the Run, Drink, Eat, Hide, and Interact houses) by latent learning during exploration. When tested in a water-deprived (WD) condition, they performed fewer errors (Figure 2d) and spent less time (Figure 2g) to reach the Drink house compared with when tested in a non-WD condition. They were injected with $A\beta_{25-35}$ peptide 2 hours after the probe test and retested after 1 week. The nontreated mice still showed a lower number of errors and lower latency to reach the goal house in WD condition, but not $A\beta_{25-35}$-treated mice (Figure 2e,h). Interestingly, while Memantine-treated $A\beta_{25-35}$ mice failed to show a difference between non-WD and WD conditions, FENM significantly restored an effective topographic memory (Figure 2e,h). Calculations of the disorientation index, as proposed by Crouzier et al. (2018) using either the errors or latencies (Figure 2f,i), confirmed that $A\beta_{25-35}$ induced a significant spatio-temporal disorientation that was completely prevented by FENM, while Memantine had no or little effects on topographic memory impairments in $A\beta_{25-35}$-injected mice (Figure 2f,i).

These data showed that both Memantine and FENM, at sub-mg/kg doses, that is, a dose level equivalent to the one proposed in humans for AD, attenuated $A\beta_{25-35}$-induced learning deficits in numerous forms of memories. As Memantine, but not FENM, showed at the highest dose tested (10 mg/kg) instead a worsening of memory abilities in the Y-maze and passive avoidance tests (Figure 1c), drugs were also tested alone in control mice. As shown in Table 2, Memantine, but not FENM, impaired learning in both tests at 10 mg/kg, suggesting some difference in the modes of action of Memantine and FENM on NMDARs.

Protective Effects of Memantine and FENM in $A\beta_{25-35}$-Injected Mice

We analyzed the protective potential of FENM compared with Memantine, against $A\beta_{25-35}$-induced memory deficits and toxicity in mice. Drugs were injected o.d. between day 1 and 7 after

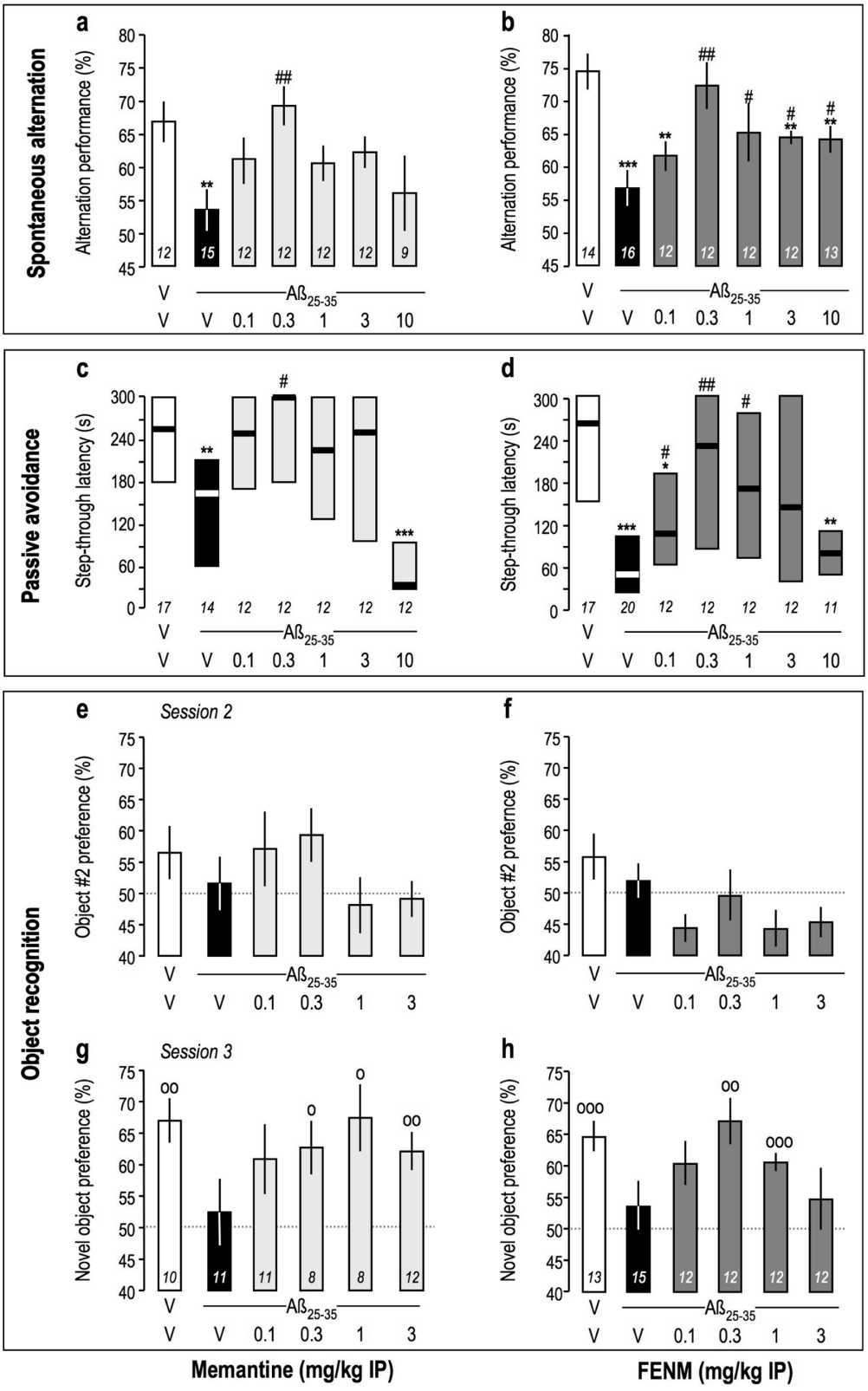

Figure 1. Anti-amnesic effect of Memantine (a, c, e, g) and FENM (b, d, f, h) on $A\beta_{25\text{-}35}$-induced learning impairments in mice: (a–b) spontaneous alternation performance, (c–d) passive avoidance, and (e–h) object recognition test. Animals received Memantine or FENM (0.1–10 mg/kg IP) 30 minutes before the Y-maze test session, passive avoidance training session, or session 2 of the object recognition test. For the object recognition test, exploration preferences are calculated with the duration of contacts in session 2 with 2 identical objects (e–f) and in session 3 with a novel object (g–h). Data show mean ± SEM (a–b, e–h) and median and interquartile range (c–d). ANOVA: $F_{(6,83)}=2.62$, $P<.05$ (a); $F_{(6,89)}=4.94$, $P<.001$ (b). Kruskal-Wallis ANOVA: $H=23.4$, $P<.001$ (c); $H=19.5$, $P<.01$ (d). *$P<.05$, **$P<.01$, ***$P<.001$ vs (Sc.Aß+V)-treated group; #$P<.05$, ##$P<.01$ vs (V+$A\beta_{25\text{-}35}$)-treated group; Dunnett's test (a–b), Dunn's test (c–d). °$P<.05$, °°$P<.01$, °°°$P<.001$ vs 50% level, 1-sample t test (g–h).

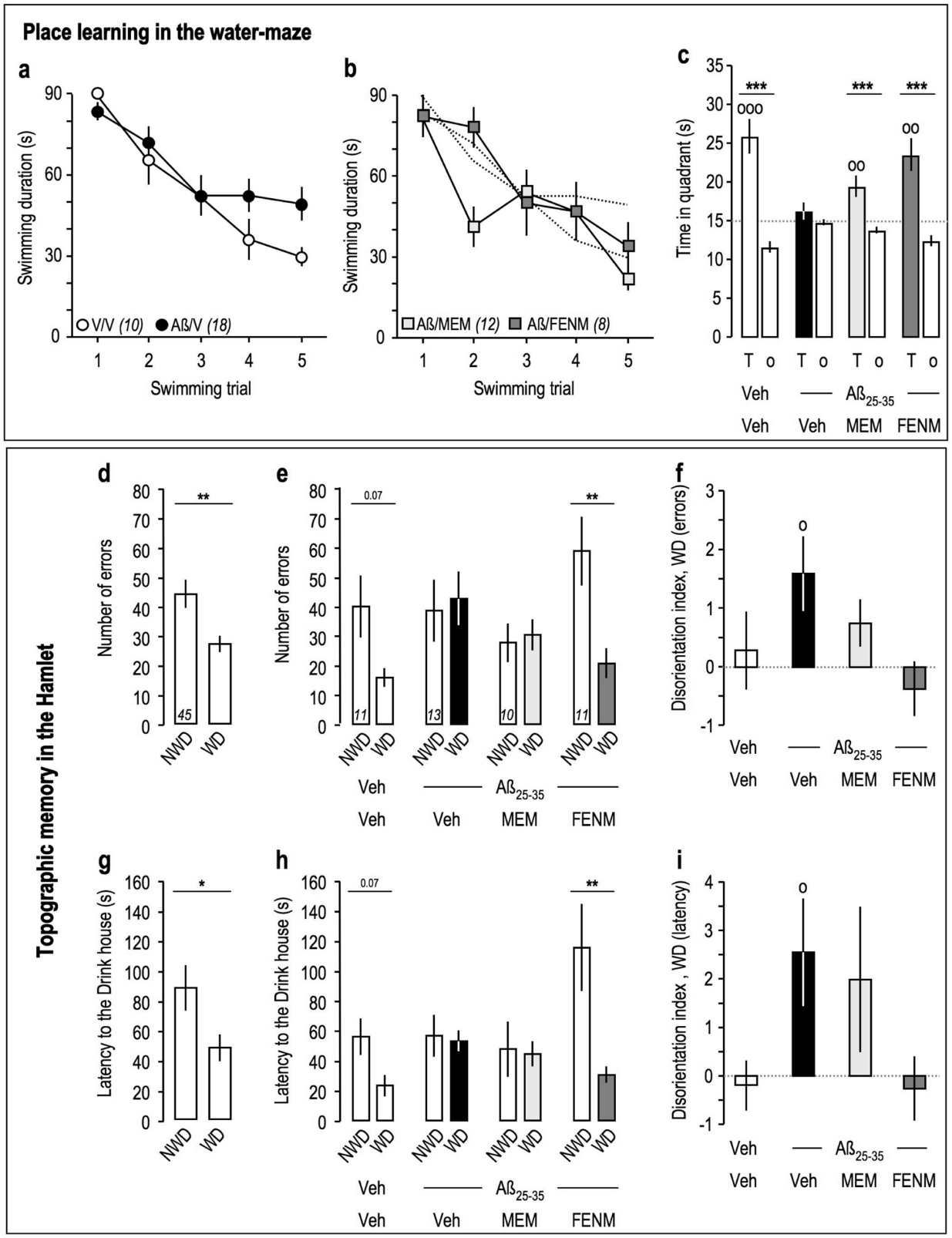

Figure 2. Effects of Memantine and FENM administered at 0.3 mg/kg IP on $A\beta_{25-35}$-induced learning impairments: (a–c) spatial reference memory in the water-maze in mice; (d–i) topographic memory in the Hamlet test. (a) Acquisition of Veh-treated and $A\beta_{25-35}$-injected animals. (b) Acquisition of animals receiving Memantine or FENM, 0.3 mg/kg IP, 30 minutes before the training trials sessions (anti-amnesia). (c) Time spent in the training (T) or the others (o) quadrants for each experimental group. °°$P < .01$, °°°$P < .001$ vs 15 seconds; 1-sample *t* test; ***$P < .001$ vs o quadrants; Student's *t* test. Hamlet probe test data were analyzed in terms of errors (d–f) and latencies (g–i) to reach the Drink house. (d, g) Probe test performed 72 hours after Hamlet training. (e, h) Probe test performed 1 week after the ICV injection of $A\beta_{25-35}$ and 30 minutes after IP injection of Memantine or FENM. (f, i) Disorientation index calculations for errors (f) or latencies (i). *$P < .05$, **$P < .01$ vs non-water deprived, paired *t* test; °$P < .05$ vs zero level, 1-sample *t* test.

Table 2. Effects of a High Dose of Memantine and FENM on Learning in Mice

Test	Saline	Memantine	FENM
		(10 mg/kg i.p.)	(10 mg/kg i.p.)
Spontaneous alternation			
Alternation (%)	70.8 ± 3.8	48.8 ± 3.0***	63.7 ± 4.2
Arm entries	30.8 ± 1.3	28.2 ± 2.9	32.7 ± 3.4
Passive avoidance			
Step-through latency (s)	300 (115–300)	26 (12–40)***	144 (103–281)
N	8	9	7

Abbreviations: FENM, fluoroethylnormemantine.
ANOVA: $F_{(2,23)} = 10.3$, $P < .001$ for alternation; $F_{(2,23)} = 0.728$, $P > .05$ for arm entries.
Kruskal-Wallis ANOVA: $H = 11.4$, $P < .01$ for step-through latency.
***$P < .001$ vs saline, Dunnett's or Dunn's test.

$A\beta_{25-35}$ and mice were tested behaviorally without further drug injection (supplemental Figure 1c). Memantine and FENM prevented $A\beta_{25-35}$-induced spontaneous alternation deficits in mice (Figure 3a–b) at doses of 0.1–3 mg/kg. The drugs also prevented $A\beta_{25-35}$-induced passive avoidance deficit in the same dose range but with significance reached at the doses of 0.1 and 1 mg/kg only for Memantine (Figure 3c), contrarily to FENM, which was active at all 0.1- to 3-mg/kg doses (Figure 3d). In the object recognition test, treatments did not affect the equal exploration of the 2 similar objects (Figure 3e–f). However, Memantine and FENM prevented $A\beta_{25-35}$-induced object recognition deficit in the same dose range, but with significance reached at the doses of 0.1 and 1 mg/kg only for Memantine (Figure 3g), contrarily to FENM, which was active at all 0.1- to 3-mg/kg doses (Figure 3h). In the water-maze test, the drugs at 0.3 mg/kg restored an acquisition profile similar to controls (Figure 4a–b), but only FENM restored a significant exploration of the T quadrant during the probe test (Figure 4c). These observations showed that on the behavioral level, Memantine and FENM protected against $A\beta_{25-35}$-induced memory impairments in mice.

Several biochemical parameters of $A\beta_{25-35}$-induced toxicity were analyzed in the mouse hippocampus or cortex. First, alteration of mitochondrial function was measured by the level of cytochrome c released into the cytosol. Cytosolic and mitochondrial fractions were isolated and the latter identified using oxphos-complex IV subunit I immunoreactivity (Figure 5a). $A\beta_{25-35}$ induced a significant increase in cytochrome c release, measured as cytosol/mitochondria content ratio, that was attenuated by Memantine and FENM (Figure 5b). A consequence of mitochondrial alteration is an increased oxidative stress and resulting peroxidation of membrane lipids. $A\beta_{25-35}$ induced a +47% increase in lipid peroxidation that was attenuated by Memantine and significantly prevented by FENM (Figure 5c).

Several markers of neuroinflammation were analyzed in hippocampus extracts. The levels of cellular markers of reactive microglia (Iba-1) or reactive astrocytes (GFAP) were moderately increased 2 weeks after $A\beta_{25-35}$ (Figure 5d–e). However, at a shorter delay of 5 days after $A\beta_{25-35}$, cytokine contents were markedly increased: +83% for IL-6 (Figure 5f) and +57% for TNFα (Figure 5g). Memantine attenuated while FENM fully prevented the increases in these cytokines (Figure 5f–g).

The treatments failed to significantly affect the levels of the anti-apoptotic protein Bcl-2, with just a trend to increased level in all $A\beta_{25-35}$ groups (Figure 5h). However, $A\beta_{25-35}$ increased the content in pro-apoptotic protein Bax by +54% (Figure 5i). Memantine and FENM significantly prevented this increase. Consequently, the Bax/Bcl-2 ratio was slightly increased by $A\beta_{25-35}$, and this increase was prevented by the drugs but only significantly by FENM (Figure 5j).

Apoptosis results in cell death, particularly in a very sensitive area like the pyramidal cell layer of the hippocampus. $A\beta_{25-35}$ injection resulted in a significant –13% decrease in viable cells stained with cresyl violet (Figure 6a–b,e) and in a +12% increase in the layer thickness, as toxicity resulted in cell swelling (Figure 6a–b,f). Memantine and FENM prevented these alterations both in terms of viable cells (Figure 6c–e) and layer thickness (Figure 6c,d,f).

Since global tissue analysis of neuroinflammatory markers by ELISA failed to show an effect of the peptide injection, neuroinflammation was also analyzed using immunohistochemistry, and several brain regions were analyzed: the stratum radiatum (Rad), molecular (Mol), and polymorph layers of the dentate gyrus (PoDG) in the hippocampus and the lateral parietal associative cortex (Figure 6g). GFAP immunolabelling in the hippocampal subfields showed an intense astroglial reaction, and cell counting showed significant increases in the Rad (Figure 7a–e) and Mol (Figure 7f–j) and a trend in PoDG (Figure 7k–o). Memantine attenuated GFAP immunolabelling in the Rad and PoDG but not Mol, while FENM showed significant prevention of $A\beta_{25-35}$-induced increases in all 3 structures (Figure 7e,j,o). Iba-1 immunolabelling was increased significantly in Rad (Figure 8a–e), showed only a marked trend in Mol (Figure 8f–j) and no change in PoDG (Figure 8k–o). Both treatments decreased $A\beta_{25-35}$-induced increases in Iba-1 labelling in Rad (Figure 8e) and showed significant decreases even compared with the V-treated group level in PoDG (Figure 8o). In the cortex, $A\beta_{25-35}$ induced significant increases in GFAP (supplemental Figure 2a–e) and Iba-1 labelling (supplemental Figure 2f–j). Memantine failed to prevent $A\beta_{25-35}$-induced increases contrarily to FENM, which showed significantly effects (supplemental Figure 2e,j).

These data show that both Memantine and FENM are protective against $A\beta_{25-35}$-induced behavioral deficits, neuroinflammation, oxidative stress, apoptosis, and cell loss, with FENM showing a more marked prevention on neuroinflammation, oxidative stress, and apoptosis parameters measured than Memantine.

Discussion

We used the pharmacological mouse model of AD induced by ICV injection of oligomeric $A\beta_{25-35}$ peptide to analyze the symptomatic and neuroprotective effects of FENM and its parent molecule, Memantine. $A\beta_{25-35}$ induced a rapid toxicity, with oxidative stress and mitochondrial alteration (Meunier et al., 2006; Lahmy et al., 2015), neuroinflammation (Rodriguez Cruz et al., 2017), apoptosis, synapse and cell loss (Maurice et al., 2013; Chumakov et al., 2015), and learning impairments (Maurice et al., 1996, 2019; Meunier et al., 2006; Lahmy et al., 2015). Moreover, $A\beta_{25-35}$ injection also activated the kinases GSK-3β, Cdk5, and MAPK, responsible for abnormal tau phosphorylation (Klementiev et al., 2007; Lahmy et al., 2013) and the secretases responsible for $A\beta_{1-42}$ protein generation (Klementiev et al., 2007; Meunier et al., 2013). Although no evidence demonstrated that tau hyperphosphorylation and increased $A\beta_{1-42}$ protein effectively contributed to the toxicity observed in the $A\beta_{25-35}$ model, the pattern of toxicity appears highly coherent with AD neurotoxicity and the model represents a coherent acute model of

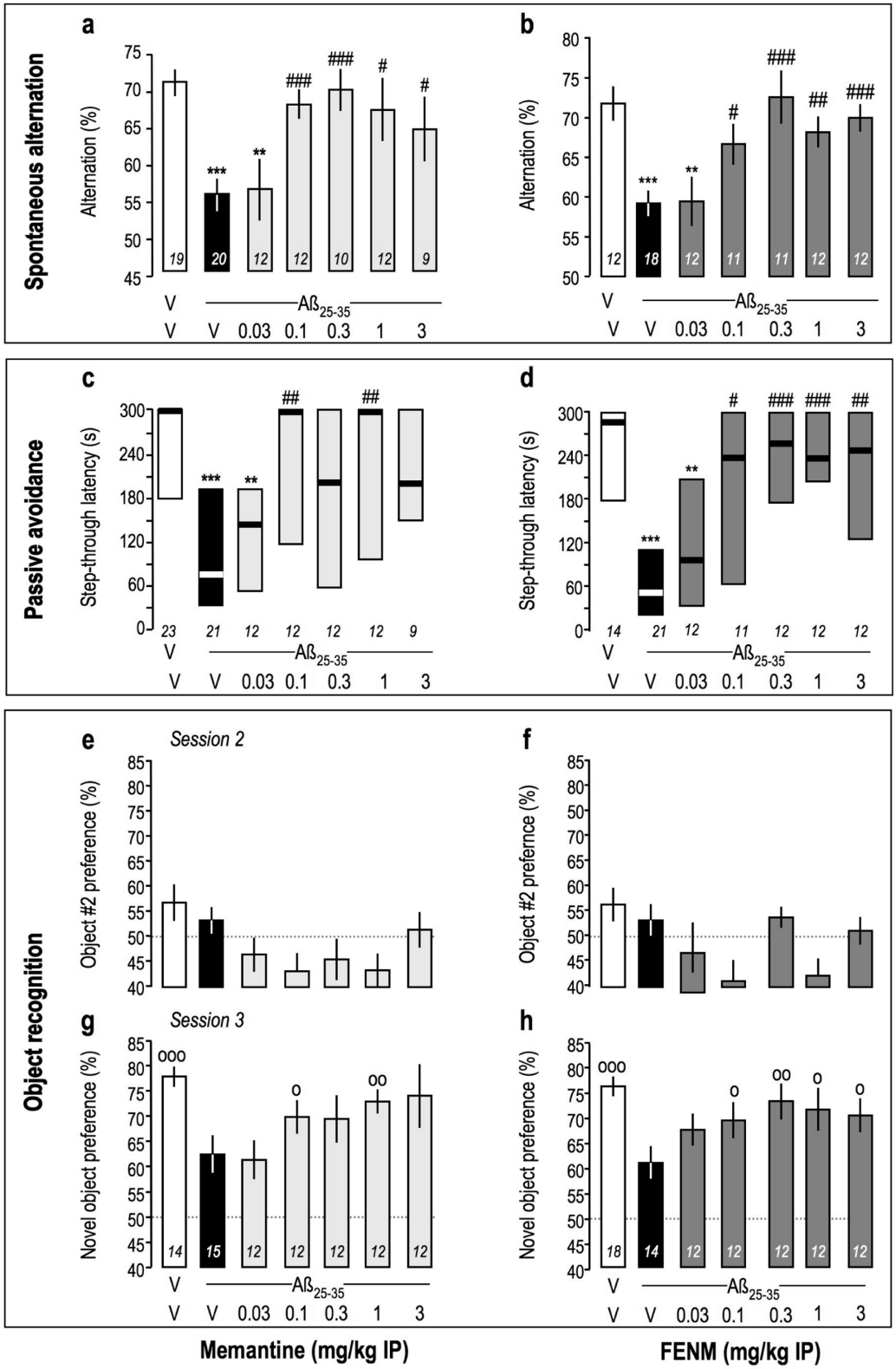

Figure 3. Protective effect of Memantine (a, c, e, g) and FENM (b, d, f, h), administered IP, on $A\beta_{25-35}$-induced learning impairments in mice: (a–b) spontaneous alternation performance, (c–d) passive avoidance, and (e–h) object recognition tests. Animals received Memantine or FENM (0.1–10 mg/kg i.p.) o.d. between day 1 to 7 and injections stopped 24 hours before the first behavioral session. For the object recognition test, exploration preferences are calculated with the duration of contacts in session 2, with 2 identical objects (e–f) and in session 3 with a novel object (g–h). Data show mean ± SEM (a, b, e–h) and median and interquartile range (c–d). ANOVA: $F_{(6,93)}=5.16$, $P<.0001$ (a); $F_{(6,90)}=6.21$, $P<.0001$ (b). Kruskal-Wallis ANOVA: $H=21.6$, $P<.01$ (c); $H=29.8$, $P<.001$ (d). $^{*}P<.05$, $^{**}P<.01$, $^{***}P<.001$ vs (V+V)-treated group; $\#P<.05$, $\#\#P<.01$ vs (V+$A\beta_{25-35}$)-treated group; Dunnett's test (a–b), Dunn's test (c–d). $^{\circ}P<.05$, $^{\circ\circ}P<.01$, $^{\circ\circ\circ}P<.001$ vs 50% level, 1-sample *t* test (g–h).

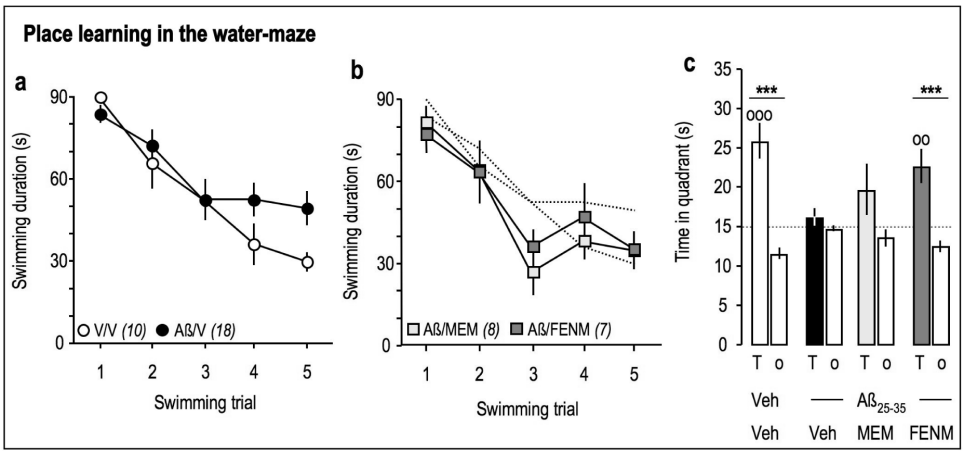

Figure 4. Protective effects of Memantine and FEN administered at 0.3 mg/kg IP on $A\beta_{25-35}$-induced learning impairments: spatial reference memory in the water-maze in mice. (a) Acquisition of Veh-treated and $A\beta_{25-35}$-injected animals. (b) Acquisition of animals receiving Memantine or FENM, 0.3 mg/kg IP, after the $A\beta_{25-35}$ peptide on day 1 and started training on day 8 (neuroprotection). (c) Time spent in the training (T) or the others (o) quadrants for each experimental group. °°$P < .01$, °°°$P < .001$ vs 15 s; 1-sample *t* test; ***$P < .001$ vs o quadrants; Student 's *t* test.

AD-like pathology. It allows the rapid and pertinent screening of symptomatic or neuroprotective drugs that will likely show efficacy after chronic treatment in transgenic mouse models of AD. For instance, a low-sialic acid form of erythropoietin injected intranasally was found active in the $A\beta_{25-35}$ model (Maurice et al., 2013) and in $hAPP_{Swe}$ mice after a 2-month chronic treatment (Rodriguez Cruz et al., 2017), and a combined therapy with baclofen and acamprosate was found as active in $A\beta_{25-35}$ mice as in $hAPP_{Swe,Lon}$ mice (Chumakov et al., 2015). The $A\beta_{25-35}$ model is therefore a suitable model to explore the therapeutic potentiality of new drugs and to compare it with clinical reference drugs such as Memantine.

We first observed that FENM and Memantine, when injected 30 minutes before the behavioral tests, reversed the $A\beta_{25-35}$-induced learning impairments. As summarized in Table 3a, Memantine and FENM were effective at doses around 0.3 mg/kg in the different tests. Memantine was effective in the 0.3- to 3-mg/kg dose range in the spontaneous alternation, passive avoidance, and object recognition tests. The drug is active at 0.3 mg/kg in the water-maze test (Table 3a). FENM also showed efficacy in the 0.1- to 1-mg/kg dose-range in the spontaneous alternation test, with a dose-response profile comparable with MEM. FENM was particularly effective in the object recognition test. The compound was also effective in the water-maze at 0.3 mg/kg. The observation that all types of memory were restored by FENM or Memantine confirmed the efficacy of the drugs to restore a functional glutamatergic neurotransmission and glutamatergic/cholinergic dialog in the hippocampus and cortex, as these neurotransmitters sustain learning processes in these different tests (Aigner, 1995). Interestingly, we observed that FENM was more effective than Memantine to restore complex memory. Indeed, the disorientation index in the Hamlet test, which measures spatial orientation and relies on both allocentric and egocentric strategies (Crouzier et al., 2018), returned to zero after FENM but not Memantine. At the tested dose of 0.3 mg/kg, FENM therefore appeared more effective on this alert sign of AD.

The drugs were then examined for their protective potency against $A\beta_{25-35}$-induced toxicity. They were administered o.d. and mice were then examined for their behavioral responses without further drug administration. Memantine was protective against $A\beta_{25-35}$-induced learning impairments in the 0.1- to 3-mg/kg dose range in the spontaneous alternation, passive avoidance, and object recognition tests (Table 3b). The dose of 0.3 mg/kg attenuated $A\beta_{25-35}$-induced place learning deficits in the water-maze but in a nonsignificant manner. FENM was also protective in the 0.1- to 3-mg/kg dose range against $A\beta_{25-35}$-induced learning impairments in all 3 tests. Furthermore, the dose of 0.3 mg/kg attenuated $A\beta_{25-35}$-induced learning deficits in the water-maze in a significant manner (Table 3b). Biochemical analyses of several markers were performed on tissue extracts. Analyses of the levels of cytochrome c release into the cytosol and of lipid peroxidation in the cortical tissue showed that Memantine nonsignificantly attenuated while FENM completely prevented $A\beta_{25-35}$-induced oxidative stress partly due to mitochondrial dysfunction (Table 3b). Bax levels were highly significantly increased by the $A\beta_{25-35}$ injection, and this increase was significantly prevented by both Memantine and FENM. Results expressed as Bax/Bcl-2 ratios confirmed the drug efficacies, but only FENM significantly decreased the $A\beta_{25-35}$-induced increase in Bax/Bcl-2 ratio. The levels of IL-6 and tumor necrosis factor-α measured at a short delay (5 days) after $A\beta_{25-35}$ showed that Memantine nonsignificantly attenuated while FENM completely prevented $A\beta_{25-35}$-induced inflammation. A precise immunofluorescence analysis of neuroinflammation was performed in several glial reacting areas of the hippocampus (Rad, Mol, PoDG), as previously described (Villard et al., 2009; Maurice et al., 2019), and in 1 cortical area taken in the same coronal plane (lateral parietal associative cortex). Both astroglial and microglial reactions were observed in the Rad and Mol areas, while the change appeared limited in PoDG. Memantine significantly attenuated astroglial reaction in Rad, but not in Mol. FENM attenuated it in both areas (Table 3b). Both drugs attenuated microglial reactions in these areas, but only FENM led to a significant difference in the Rad. In the cortex, $A\beta_{25-35}$-induced significant increases in both GFAP and Iba-1 expressed cells. Memantine marginally affected this increase while it was significantly prevented by FENM (Table 3b). FENM therefore appeared to result in a greater anti-inflammatory effect than Memantine. Neuronal cell loss was estimated in the CA1 pyramidal cell layer of the hippocampus using a viable cell staining with Cresyl violet (Villard et al., 2009; Maurice et al., 2019). The number of cells was significantly decreased by 13% after $A\beta_{25-35}$ injection, and

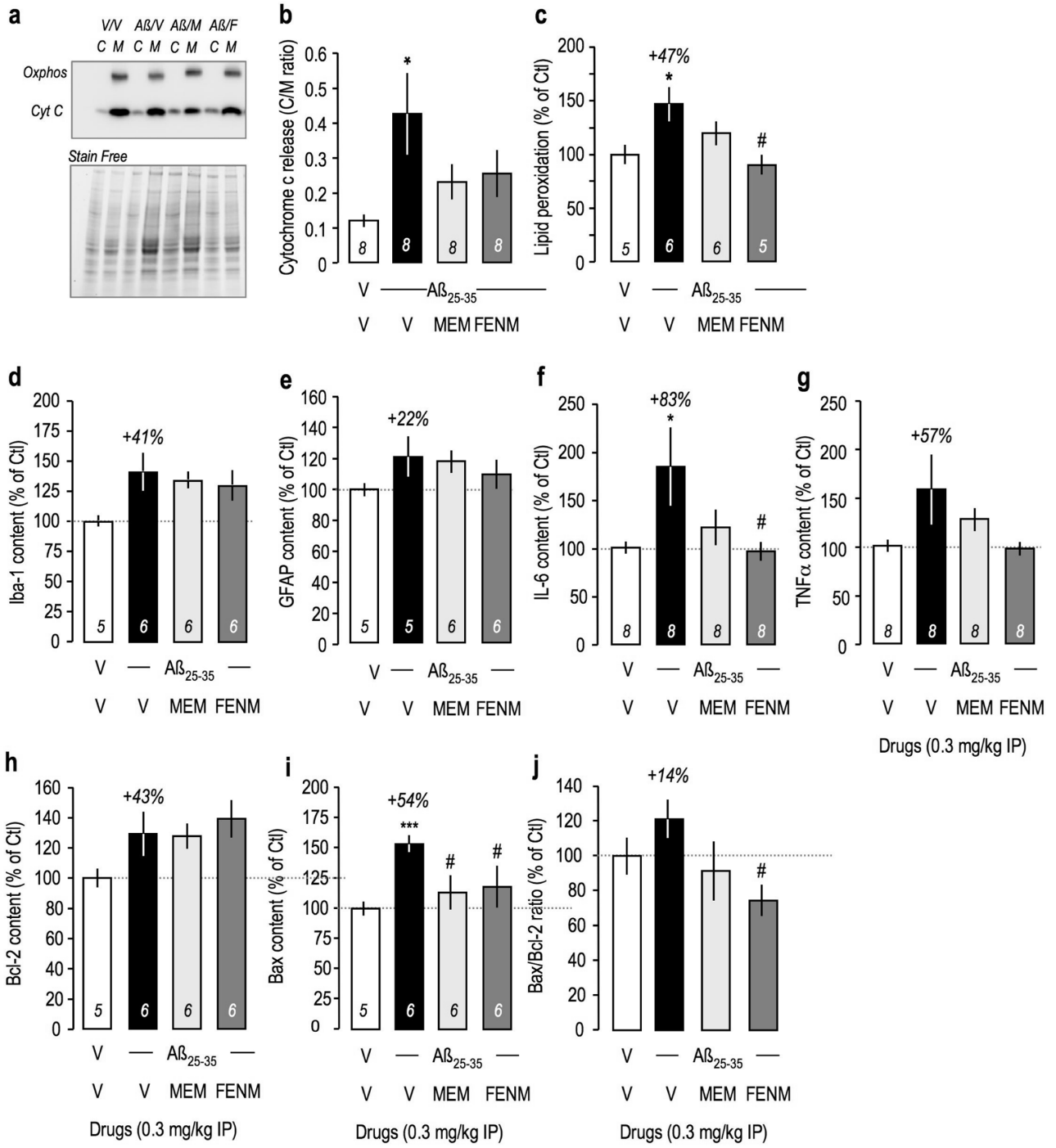

Figure 5. Protective effects of Memantine and FENM administered at 0.3 mg/kg IP on Aβ$_{25-35}$-induced (a–c) oxidative stress and mitochondrial alteration and (d) Iba-1, (e) GFAP, (f) IL-6, (g) TNFα, (h) Bcl-2, and (i) Bax contents measured by ELISA in the mouse hippocampus. (a–b) Cytochrome c release from mitochondria to the cytosol in cortex extracts. (a) Typical blots showing oxphos-complex IV subunit I mitochondrial marker and cytochrome c labeling. Normalization was done with stain free total protein content in each band. (b) Quantification. (c) Measure of lipid peroxidation level in mouse cortex extracts. ELISA assays were done 16 days after ICV injection (d–e, h–i) or 5 days after ICV injection (f–g). (j) Bax/Bcl-2 ratio. ANOVA: $F_{(3,31)}=3.05$, $P<.05$ (b). $F_{(3,21)}=4.33$, $P<.05$; $F_{(3,22)}=2.53$, $P>.05$ (d); $F_{(3,21)}=1.06$, $P>.05$ (e); $F_{(3,31)}=3.06$, $P<.05$ (f); $F_{(3,31)}=2.10$, $P>.05$ (g); $F_{(3,22)}=2.00$, $P>.05$ (h); $F_{(3,22)}=3.37$, $P<.05$ (i); $F_{(3,22)}=0.763$, $P>.05$ (j). *$P<.05$, ***$P<.001$ vs (V+V)-treated group; #$P<.05$ vs (V+Aβ$_{25-35}$)-treated group; Dunnett's test.

the remaining cells markedly swelled, thus increasing the layer thickness by 12%. Both Memantine and FENM significantly prevented cell loss and layer thickening.

These observations confirmed previous data showing that Memantine is neuroprotective in preclinical rodent models of AD. This was observed in the Aβ$_{25-35}$ model, the drug attenuating learning impairments, changes in neuropeptides, enzymes, glial markers, and iNOS activity induced by the peptide (Arif and Kato, 2009; Arif et al., 2009; Maurice, 2016). Wang et al. (2015) reported that in a rat model of AD induced by ICV

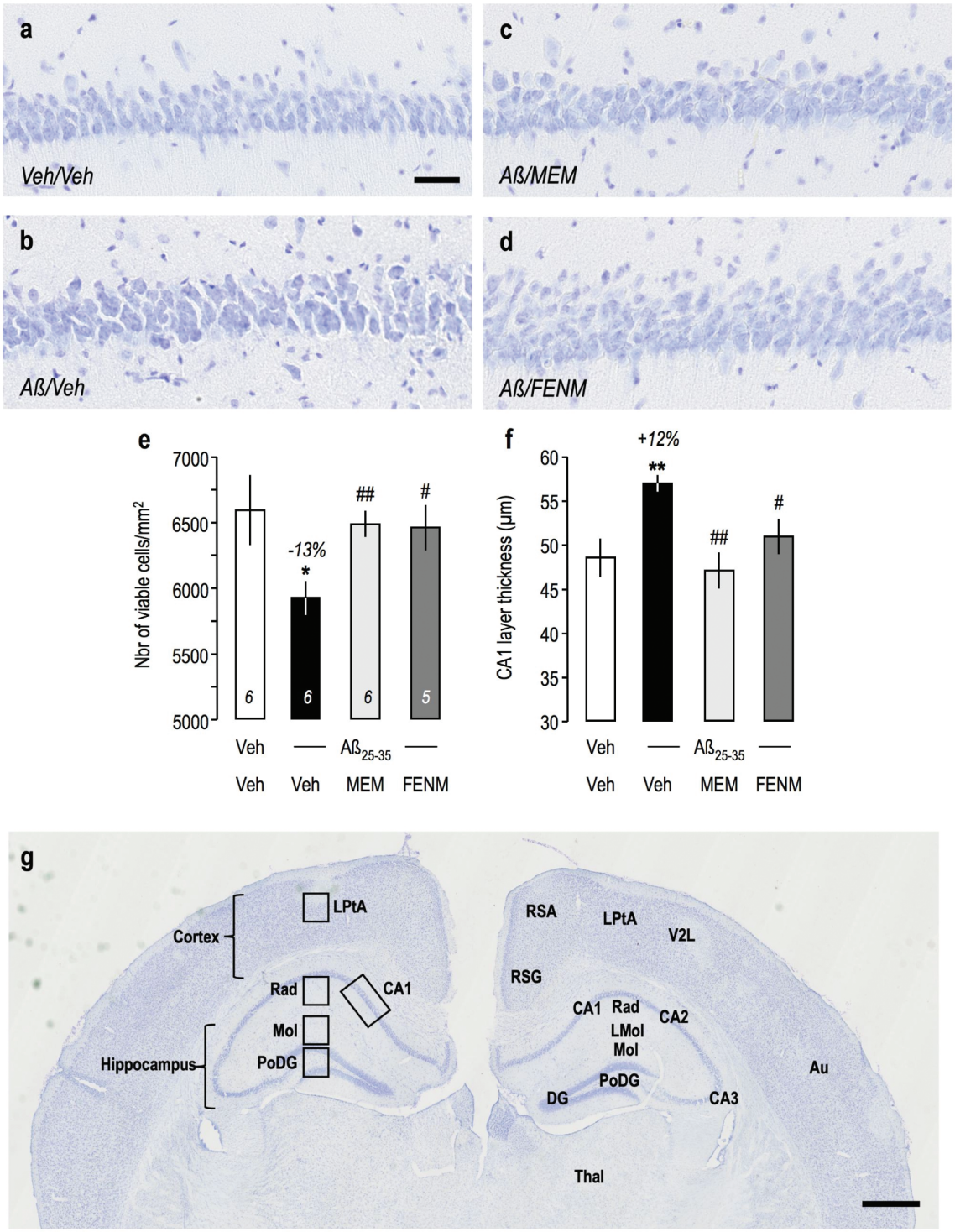

Figure 6. Protective effects of Memantine and FENM administered at 0.3 mg/kg IP on cell loss in the CA1 hippocampal pyramidal cell layer of $A\beta_{25-35}$-treated mice using cresyl violet staining: (a–d) typical micrographs and (e) quantifications of the number of viable cells and (f) the cell layer thickness. 3–6 slices were counted per animals. ANOVA: $F_{(3,113)}=9.08$, $P<.0001$ (i); $F_{(3,113)}=8.35$, $P<.0001$ (j). *$P<.05$, **$P<.01$ vs the (V+V)-treated group; #$P<.05$, ##$P<.01$ vs the ($A\beta_{25-35}$+V)-treated group; Dunnett's test. (g) Anatomical localization of the hippocampal and cortical areas analyzed in the mouse brain (cresyl violet staining at low magnification). Left: areas; right: anatomical distribution. Abbreviations: Au, 2nd auditory cortex; CA1~CA3, pyramidal cell layers; DG, dentate gyrus; LMol, lacunosum molecular layer; LPtA, lateral parietal associative cortex; Mol, molecular layer of the DG; PoDG, polymorph layer of the DG; Rad, stratum radiatum; RSG, retrosplenial granular cortex; RSA, retroplenial agranular cortex; Thal, thalamus; V2L, lateral area of the 2nd visual cortex. Scale bars = 50 µm (a), 500 µm (g).

injection of an adeno-associated viral vector overexpressing the protein phosphatase-2A inhibitor, Memantine at 2 mg/kg/d orally during 6 weeks rescued protein phosphatase-2A activity and attenuated AD-like pathology and cognitive deficits in the rats. In transgenic models, the drug showed symptomatic and neuroprotective effects in the $hAPP_{Swe}$, APP/PS1, APP23, and

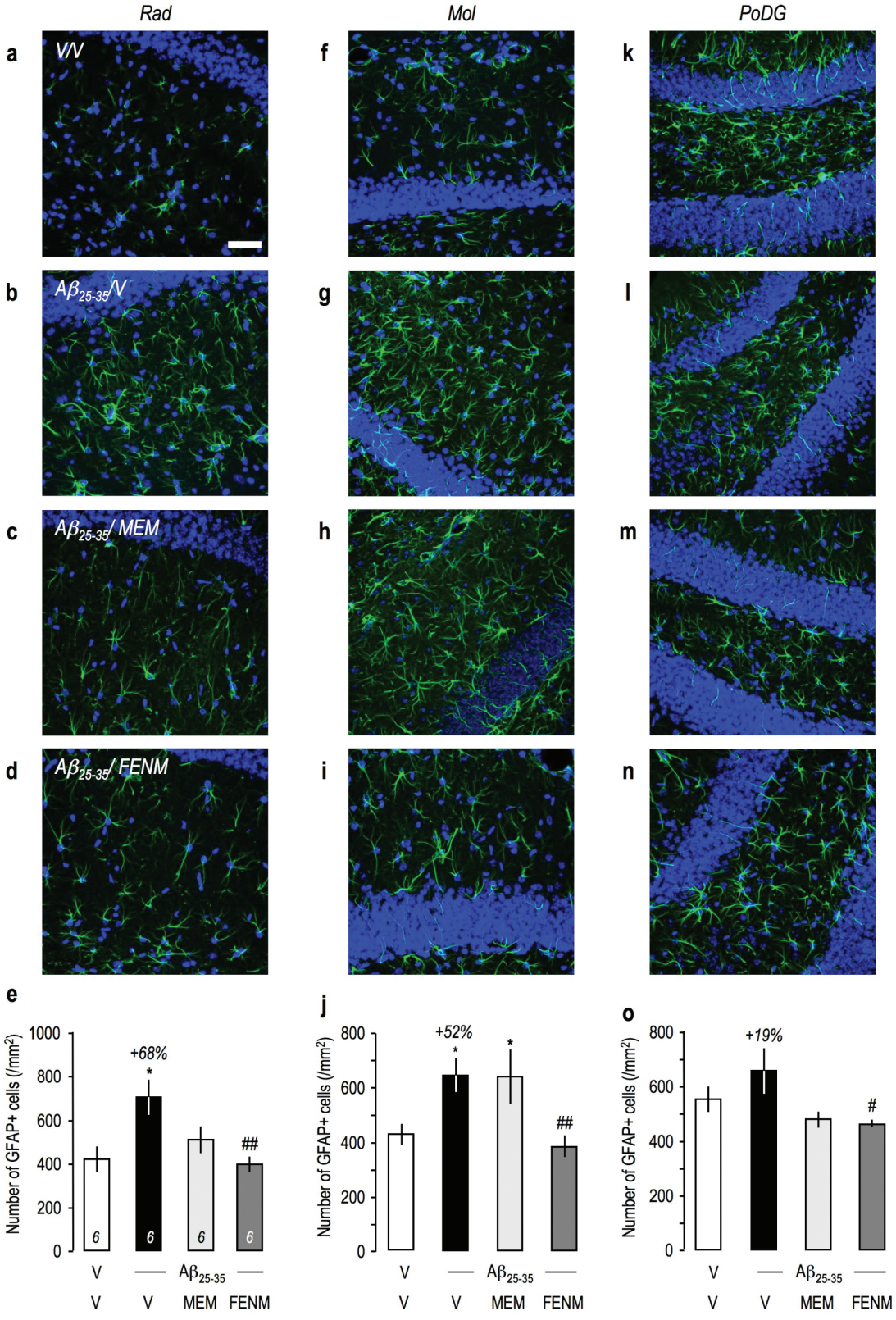

Figure 7. Protective effects of Memantine and FENM administered at 0.3 mg/kg IP on the astroglial reaction in the hippocampus of Aβ$_{25-35}$-treated mice using GFAP immunolabeling: (a–e) stratum radiatum, (f–j) molecular layer, and (k–o) polymorph layer with (a–d, f–i, k–n) typical immunofluorescence micrographs (blue: DAPI, green: GFAP) and (e, j, o) quantifications. Coronal 25-µm-thick sections were stained with anti-GFAP antibody and 3 areas of the hippocampus analyzed as shown in Figure 8g. Scale bar (a) = 50 µm. ANOVA: $F_{(3,22)} = 5.06$, $P < .01$ (e); $F_{(3,23)} = 4.50$, $P < .05$ (j); $F_{(3,23)} = 3.24$, $P < .05$ (o). *$P < .05$, ***$P < .001$ vs the (V+V)-treated group; #$P < .05$, ##$P < .01$ vs the (Aβ$_{25-35}$+V)-treated group; Dunnett's test.

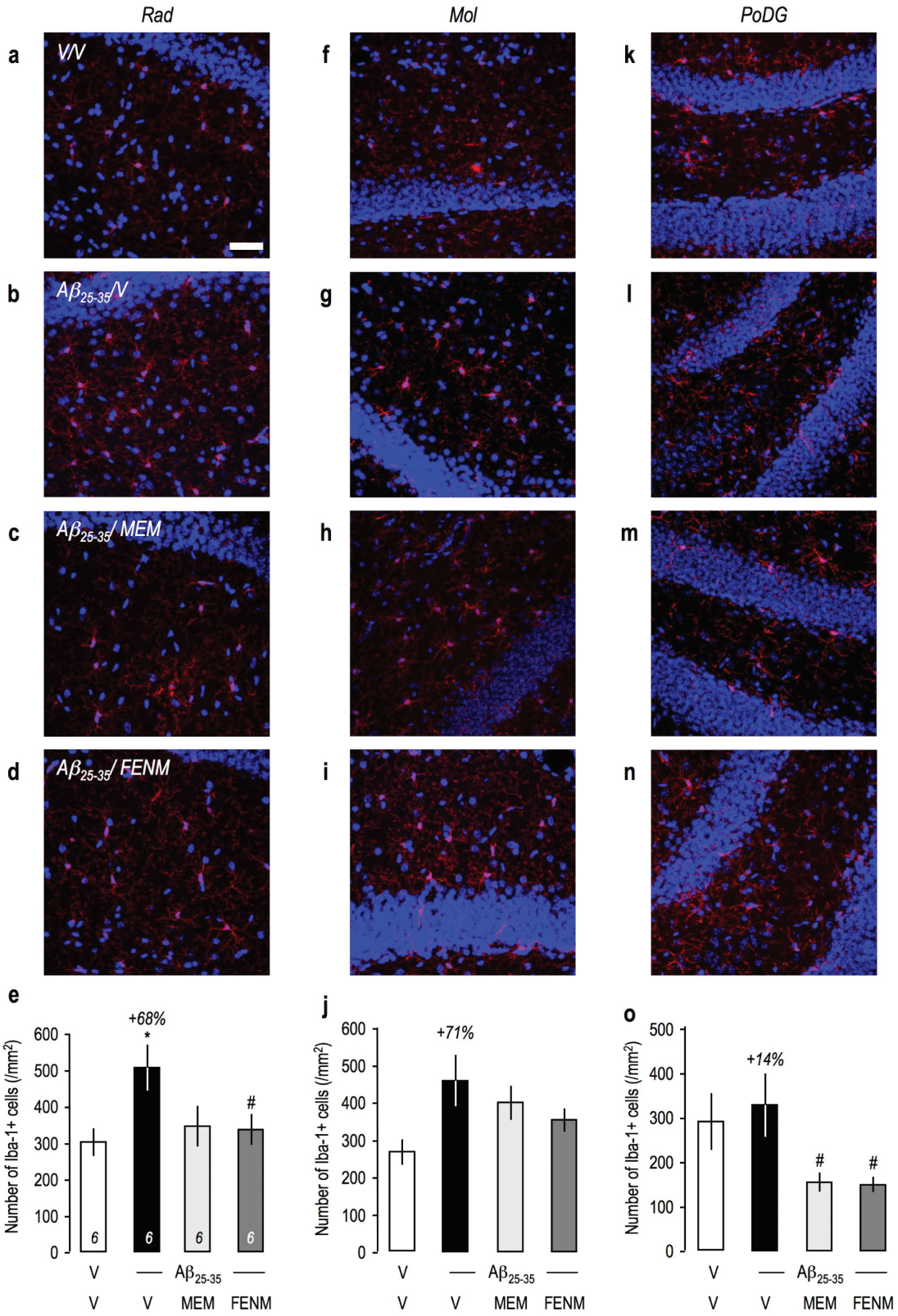

Figure 8. Protective effects of Memantine and FENM administered at 0.3 mg/kg IP on the microglial reaction in the hippocampus of $A\beta_{25-35}$-treated mice using Iba-1 immunolabeling: (a–e) stratum radiatum, (f–j) molecular layer, and (k–o) polymorph layer with (a–d, f–i, k–n) typical immunofluorescence micrographs (blue: DAPI, red: Iba-1) and (e, j, o) quantifications. Coronal 25-µm-thick sections were stained with anti-Iba-1 antibody and 3 areas of the hippocampus analyzed as shown in Figure 6g. Scale = 50 µm. ANOVA: $F_{(3,23)} = 3.22$, $P < .05$ (e); $F_{(3,22)} = 2.86$, $P > .05$ (j); $F_{(3,23)} = 3.38$, $P < .05$ (o). $^{*}P < .05$, $^{***}P < .001$ vs the (V+V)-treated group; $\#P < .05$, $\#\#P < .01$ vs the ($A\beta_{25-35}$+V)-treated group; Dunnett's test.

Table 3. Active Dose Range or Observed Effects in the Analysis of the Anti-Amnesic or Neuroprotective Effect of FENM in the $A\beta_{25-35}$ Mouse Model of AD

Parameter	FENM	Memantine
(a) Anti-amnesia		
Behavioral analyses[a]		
Spontaneous alternation	0.3–10	0.3
Passive avoidance	0.1–1	0.3
Object recognition	0.3–1	0.3–3
Water-maze	0.3	0.3
Topographic memory	++	–
Amnesic effect alone (SA, PA)	–	10
(b) Neuroprotection		
Behavioral analyses[a]		
Spontaneous alternation	0.1–3	0.1–3
Passive avoidance	0.1–3	0.1–1
Object recognition	0.1–3	0.1–3
Water-maze	0.3	–
Biochemical analyses[b]		
Cyt C release	+	+
Lipid peroxidation	++	+
IL-6 ELISA	++	+
TNFα ELISA	+	+
Bax/Bcl2 ELISA	++	+
Morphological analyses[b]		
Pyramidal cell loss (CV)	++	++
GFAP IHC—Rad	++	+
GFAP IHC—Mol	++	–
GFAP IHC—PoDG	++	+
GFAP IHC—Ctx	++	–
Iba1 IHC—Rad	++	+
Iba1 IHC—Ctx	++	–

Abbreviations: –, no effect; +, attenuation; ++, prevention; CV, cresyl violet; Cyt c, cytochrome c; ELISA, enzyme-linked immune-sorbent assay; FENM, fluoroethylnormemantine; IHC, immunohistochemistry; Mol, molecular layer of the hippocampus; PA, passive avoidance; PoDG, polymorph layer of the dentate gyrus; Rad, stratum radiatum; SA, spontaneous alternation.
*a*Active dose range (in mg/kg i.p.).
*b*All parameters tested at the active dose of 0.3 mg/kg i.p. – (not significant vs $A\beta_{25-35}$ +V group). + (not significant vs V+V group but not significant vs $A\beta_{25-35}$+V group). ++ (significant vs $A\beta_{25-35}$+V group).

3xTg-AD lines (Minkevicienne et al., 2004; Van Dam et al., 2005; Van Dam and De Deyn, 2006; Dong et al., 2008). So, contrarily to its use in clinic resulting in limited symptomatic effects, Memantine coherently led to symptomatic and neuroprotective effect in preclinical models.

The biochemical and morphological analyses showed that the novel derivative FENM induced a more clear-cut neuroprotection, particularly on oxidative stress and apoptosis markers and on neuroinflammation markers in the hippocampus and cortex. The drug acts as its parent molecule as a weak noncompetitive NMDAR antagonist. Although the precise mode of action of FENM needs to be further refined using adequate electrophysiological analyses, the drug labeled NMDARs in the brain when it was used as a PET radiotracer (Salabert et al., 2015, 2018). The mechanism of action of Memantine was also found to involve several cellular regulation pathways beyond its effect at NMDARs. The drug protected against Aβ oligomer-induced reactive oxygen species formation (De Felice et al., 2007), stimulated cholinergic signaling through muscarinic acetylcholine receptors (Drever et al., 2007), regulated nerve growth factor signaling by increasing TrkA activation and decreasing p75NTR signaling (Liu et al., 2014), and regulated protein phosphatase-2A activation (Wang et al., 2015). FENM likely shares these different effects in AD mice, but the drug appeared more effective in preventing oxidative stress and neuroinflammation and failed to induced learning deficits at a high dose (10 mg/kg). FENM may therefore present additional targets or a slightly different mechanism of action NMDARs that deserve to be analyzed.

FENM appeared as a promising drug. Its effect must now be confirmed in transgenic mouse models of AD. Only repeated administration regimens in these chronic models will allow to determine if FENM is able to decrease the amyloid load and plaque formation in amyloid-based models or kinases activities and neurofibrillary tangles formation in tau-based models. This was previously described for Memantine (Wang et al., 2015) and several other drugs with similar symptomatic and neuroprotective profiles. The strength of FENM-induced neuroprotection must be investigated in similar transgenic models in the future, in parallel to the analysis of the drug mechanism of action, to establish the superiority of the molecule over Memantine and to determine whether the drug is a putative candidate for synergic combinations with current drugs under development.

In conclusion, we described the symptomatic and neuroprotective efficacy of a novel Memantine derivative, FENM, in a pharmacological mouse model of AD. Comparison with its parent molecule revealed that FENM is more effective in preventing oxidative stress, apoptosis, and neuroinflammation and suggested that the molecule may not only be used as a potent PET radiotracer for NMDAR but also as a promising neuroprotective drug in AD. Moreover, the compound may be used at more relevant dosages than those actually proposed with the Memantine treatment.

Supplementary Materials

Supplementary data are available at *International Journal of Neuropsychopharmacology (IJNPPY)* online.

Significance Statement

Currently available therapeutic strategies in Alzheimer's disease show limited efficacy, particularly in terms of long-lasting neuroprotection and potential disease-modifying action. Among clinical drugs, Memantine is a noncompetitive NMDA receptor antagonist with marked anti-hypoxic and synapse-stabilizing effects. We here described a memantine derivative, Fluoroethylnormemantine (FENM), with superior pharmacological efficacy than its parent molecule. The drug showed potent symptomatic and neuroprotective effects in a pharmacological mouse model of Alzheimer's disease with no amnesic effect by itself at a high dose. The drug, already used as a PET radiotracer, deserves to be further developed as a novel neuroprotective agent.

Acknowledgments

The authors thank Marc Criton and Lorène Milliex (SATT AxLR, Montpellier, France) for regular advice during the project; Dr Christine Denny (University of Columbia, NY) for careful reading of the manuscript; M2i Life Sciences for providing FENM; and the CECEMA animal facility of the University of Montpellier.

T. Maurice designed the study; S. Couly and G. Rubinstenn amended the study design; S. Couly, M. Denus and M. Bouchet performed the behavioral, immunohistochemical, and biochemical analyses; S. Couly and T. Maurice analyzed the data. T. Maurice wrote the draft version of the manuscript; S. Couly

and G. Rubinstenn corrected the manuscript. All authors approved the final version.

This work was supported by a grant from SATT AxLR (FR-2005–138) to T. Maurice.

Interest Statement

G. Rubinstenn is co-inventor and owner of the patent FR-2005–138 pending and is founder of ReST Therapeutics. T. Maurice is co-inventor of the patent FR-2005–138 pending. Other authors declare no conflict of interest.

References

Aigner TG (1995) Pharmacology of memory: cholinergic-glutamatergic interactions. Curr Opin Neurobiol 5:155–160.

Ametamey SM, Samnick S, Leenders KL, Vontobel P, Quack G, Parsons CG, Schubiger PA (1999) Fluorine-18 radiolabelling, biodistribution studies and preliminary PET evaluation of a new memantine derivative for imaging the NMDA receptor. J Recept Signal Transduct Res 19:129–141.

Ametamey SM, Bruehlmeier M, Kneifel S, Kokic M, Honer M, Arigoni M, Buck A, Burger C, Samnick S, Quack G, Schubiger PA (2002) PET studies of 18F-memantine in healthy volunteers. Nucl Med Biol 29:227–231.

Arif M, Chikuma T, Ahmed MM, Nakazato M, Smith MA, Kato T (2009) Effects of memantine on soluble Alphabeta(25-35)-induced changes in peptidergic and glial cells in Alzheimer's disease model rat brain regions. Neuroscience 164:1199–1209.

Arif M, Kato T (2009) Increased expression of PAD2 after repeated intracerebroventricular infusions of soluble Abeta(25-35) in the Alzheimer's disease model rat brain: effect of memantine. Cell Mol Biol Lett 14:703–714.

Avila J, Llorens-Martín M, Pallas-Bazarra N, Bolós M, Perea JR, Rodríguez-Matellán A, Hernández F (2017) Cognitive decline in neuronal aging and Alzheimer's disease: role of NMDA receptors and associated proteins. Front Neurosci 11:626.

Beconi MG, Howland D, Park L, Lyons K, Giuliano J, Dominguez C, Munoz-Sanjuan I, Pacifici R (2011) Pharmacokinetics of memantine in rats and mice. PLoS Curr 3:RRN1291.

Bloom GS (2014) Amyloid-β and tau: the trigger and bullet in Alzheimer disease pathogenesis. JAMA Neurol 71:505–508.

Bondi MW, Edmonds EC, Salmon DP (2017) Alzheimer's disease: past, present, and future. J Int Neuropsychol Soc 23:818–831.

Brookmeyer R, Gray S, Kawas C (1998) Projections of Alzheimer's disease in the United States and the public health impact of delaying disease onset. Am J Public Health 88:1337–1342.

Butterfield DA, Halliwell B (2019) Oxidative stress, dysfunctional glucose metabolism and Alzheimer disease. Nat Rev Neurosci 20:148–160.

Chumakov I, Nabirotchkin S, Cholet N, Milet A, Boucard A, Toulorge D, Pereira Y, Graudens E, Traoré S, Foucquier J, Guedj M, Vial E, Callizot N, Steinschneider R, Maurice T, Bertrand V, Scart Grès C, Hajj R, Cohen D (2015) Combining two repurposed drugs as a promising approach for Alzheimer's disease therapy. Sci Rep 5:7608.

Crouzier L, Gilabert D, Rossel M, Trousse F, Maurice T (2018) Topographical memory analyzed in mice using the Hamlet test, a novel complex maze. Neurobiol Learn Mem 149:118–134.

Crouzier L, Maurice T (2018) Assessment of topographic memory in mice in a complex environment using the hamlet test. Curr Protoc Mouse Biol 8:e43.

Danysz W, Parsons CG (2003) The NMDA receptor antagonist memantine as a symptomatological and neuroprotective treatment for Alzheimer's disease: preclinical evidence. Int J Geriatr Psychiatry 18:S23–S32.

De Felice FG, Velasco PT, Lambert MP, Viola K, Fernandez SJ, Ferreira ST, Klein WL (2007) Abeta oligomers induce neuronal oxidative stress through an N-methyl-D-aspartate receptor-dependent mechanism that is blocked by the Alzheimer drug memantine. J Biol Chem 282:11590–11601.

Deardorff WJ, Grossberg GT (2016) Pharmacotherapeutic strategies in the treatment of severe Alzheimer's disease. Expert Opin Pharmacother 17:1789–1800.

Dong H, Yuede CM, Coughlan C, Lewis B, Csernansky JG (2008) Effects of memantine on neuronal structure and conditioned fear in the Tg2576 mouse model of Alzheimer's disease. Neuropsychopharmacology 33:3226–3236.

Drever BD, Anderson WG, Johnson H, O'Callaghan M, Seo S, Choi DY, Riedel G, Platt B (2007) Memantine acts as a cholinergic stimulant in the mouse hippocampus. J Alzheimers Dis 12:319–333.

Ettcheto M, Sánchez-López E, Gómez-Mínguez Y, Cabrera H, Busquets O, Beas-Zarate C, García ML, Carro E, Casadesus G, Auladell C, Vázquez Carrera M, Folch J, Camins A (2018) Peripheral and central effects of memantine in a mixed preclinical mice model of obesity and familial Alzheimer's disease. Mol Neurobiol 55:7327–7339.

Folch J, Busquets O, Ettcheto M, Sánchez-López E, Castro-Torres RD, Verdaguer E, Garcia ML, Olloquequi J, Casadesús G, Beas-Zarate C, Pelegri C, Vilaplana J, Auladell C, Camins A (2018) Memantine for the treatment of dementia: a review on its current and future applications. J Alzheimers Dis 62:1223–1240.

Frost B, Jacks RL, Diamond MI (2009) Propagation of tau misfolding from the outside to the inside of a cell. J Biol Chem 284:12845–12852.

Hardingham GE, Bading H (2010) Synaptic versus extrasynaptic NMDA receptor signalling: implications for neurodegenerative disorders. Nat Rev Neurosci 11:682–696.

Kilkenny C, Browne W, Cuthill IC, Emerson M, Altman DG; NC3Rs Reporting Guidelines Working Group (2010) Animal research: reporting in vivo experiments: the ARRIVE guidelines. Br J Pharmacol 160:1577–1579.

Klementiev B, Novikova T, Novitskaya V, Walmod PS, Dmytriyeva O, Pakkenberg B, Berezin V, Bock E (2007) A neural cell adhesion molecule-derived peptide reduces neuropathological signs and cognitive impairment induced by Abeta25-35. Neuroscience 145:209–224.

Lahmy V, Meunier J, Malmström S, Naert G, Givalois L, Kim SH, Villard V, Vamvakides A, Maurice T (2013) Blockade of Tau hyperphosphorylation and $A\beta_{1\text{-}42}$ generation by the aminotetrahydrofuran derivative ANAVEX2-73, a mixed muscarinic and σ_1 receptor agonist, in a nontransgenic mouse model of Alzheimer's disease. Neuropsychopharmacology 38:1706–1723.

Lahmy V, Long R, Morin D, Villard V, Maurice T (2015) Mitochondrial protection by the mixed muscarinic/σ1 ligand ANAVEX2-73, a tetrahydrofuran derivative, in Aβ25-35 peptide-injected mice, a nontransgenic Alzheimer's disease model. Front Cell Neurosci 8:463.

Lang UE, Mühlbacher M, Hesselink MB, Zajaczkowski W, Danysz W, Danker-Hopfe H, Hellweg R (2004) No nerve growth factor response to treatment with memantine in adult rats. J Neural Transm (Vienna) 111:181–190.

Liu MY, Wang S, Yao WF, Zhang ZJ, Zhong X, Sha L, He M, Zheng ZH, Wei MJ (2014) Memantine improves spatial learning and memory impairments by regulating NGF signaling in APP/PS1 transgenic mice. Neuroscience 273:141–151.

Maurice T (2016) Protection by sigma-1 receptor agonists is synergic with donepezil, but not with memantine, in a mouse model of amyloid-induced memory impairments. Behav Brain Res 296:270–278.

Maurice T, Lockhart BP, Privat A (1996) Amnesia induced in mice by centrally administered beta-amyloid peptides involves cholinergic dysfunction. Brain Res 706:181–193.

Maurice T, Mustafa MH, Desrumaux C, Keller E, Naert G, de la C. García-Barceló M, Rodríguez Cruz Y, Garcia Rodríguez JC (2013) Intranasal formulation of erythropoietin EPO) showed potent protective activity against amyloid toxicity in the $A\beta_{25-35}$ nontransgenic mouse model of Alzheimer's disease. J Psychopharmacol. 27:1044–57.

Maurice T, Volle JN, Strehaiano M, Crouzier L, Pereira C, Kaloyanov N, Virieux D, Pirat JL (2019) Neuroprotection in non-transgenic and transgenic mouse models of Alzheimer's disease by positive modulation of σ1 receptors. Pharmacol Res 144:315–330.

Meunier J, Ieni J, Maurice T (2006) The anti-amnesic and neuroprotective effects of donepezil against amyloid beta25-35 peptide-induced toxicity in mice involve an interaction with the sigma1 receptor. Br J Pharmacol 149:998–1012.

Meunier J, Villard V, Givalois L, Maurice T (2013) The γ-secretase inhibitor 2-[(1R)-1-[(4-chlorophenyl)sulfonyl] (2,5-difluorophenyl) amino]ethyl-5-fluorobenzenebutanoic acid (BMS-299 897) alleviates Aβ1-42 seeding and short term memory deficits in the Aβ25-35 mouse model of Alzheimer's disease. Eur J Pharmacol 698:193–199.

Minkeviciene R, Banerjee P, Tanila H (2004) Memantine improves spatial learning in a transgenic mouse model of Alzheimer's disease. J Pharmacol Exp Ther 311:677–682.

Misztal M, Frankiewicz T, Parsons CG, Danysz W (1996) Learning deficits induced by chronic intraventricular infusion of quinolinic acid–protection by MK-801 and memantine. Eur J Pharmacol 296:1–8.

Mota SI, Ferreira IL, Rego AC (2014) Dysfunctional synapse in Alzheimer's disease - a focus on NMDA receptors. Neuropharmacology 76 Pt A:16–26.

Nakamura S, Murayama N, Noshita T, Katsuragi R, Ohno T (2006) Cognitive dysfunction induced by sequential injection of amyloid-beta and ibotenate into the bilateral hippocampus; protection by memantine and MK-801. Eur J Pharmacol 548:115–122.

Patel L, Grossberg GT (2011) Combination therapy for Alzheimer's disease. Drugs Aging 28:539–546.

Paxinos G, Franklin KBJ (2004) The mouse brain in stereotaxic coordinates. San Diego, CA: Academic Press.

Pike CJ, Burdick D, Walencewicz AJ, Glabe CG, Cotman CW (1993) Neurodegeneration induced by beta-amyloid peptides in vitro: the role of peptide assembly state. J Neurosci 13:1676–1687.

Rodríguez Cruz Y, Strehaiano M, Rodríguez Obaya T, García Rodríguez JC, Maurice T (2017) An intranasal formulation of erythropoietin (Neuro-EPO) prevents memory deficits and amyloid toxicity in the APPSwe transgenic mouse model of Alzheimer's disease. J Alzheimers Dis 55:231–248.

Rosi S, Vazdarjanova A, Ramirez-Amaya V, Worley PF, Barnes CA, Wenk GL (2006) Memantine protects against LPS-induced neuroinflammation, restores behaviorally-induced gene expression and spatial learning in the rat. Neuroscience 142:1303–1315.

Salabert AS, Fonta C, Fontan C, Adel D, Alonso M, Pestourie C, Belhadj-Tahar H, Tafani M, Payoux P (2015) Radiolabeling of [18F]-fluoroethylnormemantine and initial in vivo evaluation of this innovative PET tracer for imaging the PCP sites of NMDA receptors. Nucl Med Biol 42:643–653.

Salabert AS, Mora-Ramirez E, Beaurain M, Alonso M, Fontan C, Tahar HB, Boizeau ML, Tafani M, Bardiès M, Payoux P (2018) Evaluation of [18F]FNM biodistribution and dosimetry based on whole-body PET imaging of rats. Nucl Med Biol 59:1–8.

Salomone S, Caraci F, Leggio GM, Fedotova J, Drago F (2012) New pharmacological strategies for treatment of Alzheimer's disease: focus on disease modifying drugs. Br J Clin Pharmacol 73:504–517.

Samnick S, Ametamey S, Leenders KL, Vontobel P, Quack G, Parsons CG, Neu H, Schubiger PA (1998) Electrophysiological study, biodistribution in mice, and preliminary PET evaluation in a rhesus monkey of 1-amino-3-[18F]fluoromethyl-5-methyl-adamantane (18F-MEM): a potential radioligand for mapping the NMDA-receptor complex. Nucl Med Biol 25:323–330.

Selkoe DJ (1991) The molecular pathology of Alzheimer's disease. Neuron 6:487–498.

Selkoe DJ (2004) Cell biology of protein misfolding: the examples of Alzheimer's and Parkinson's diseases. Nat Cell Biol 6:1054–1061.

Valis M, Herman D, Vanova N, Masopust J, Vysata O, Hort J, Pavelek Z, Klimova B, Kuca K, Misik J, Zdarova Karasova J (2019) The concentration of memantine in the cerebrospinal fluid of Alzheimer's disease patients and its consequence to oxidative stress biomarkers. Front Pharmacol 10:943.

Van Dam D, Abramowski D, Staufenbiel M, De Deyn PP (2005) Symptomatic effect of donepezil, rivastigmine, galantamine and memantine on cognitive deficits in the APP23 model. Psychopharmacology (Berl) 180:177–190.

Van Dam D, De Deyn PP (2006) Cognitive evaluation of disease-modifying efficacy of galantamine and memantine in the APP23 model. Eur Neuropsychopharmacol 16:59–69.

Villard V, Espallergues J, Keller E, Alkam T, Nitta A, Yamada K, Nabeshima T, Vamvakides A, Maurice T (2009) Antiamnesic and neuroprotective effects of the aminotetrahydrofuran derivative ANAVEX1-41 against amyloid beta(25-35)-induced toxicity in mice. Neuropsychopharmacology 34:1552–1566.

Villard V, Espallergues J, Keller E, Vamvakides A, Maurice T (2011) Anti-amnesic and neuroprotective potentials of the mixed muscarinic receptor/sigma$_1$ (σ_1) ligand ANAVEX2-73, a novel aminotetrahydrofuran derivative. J Psychopharmacol. 25:1101–1117.

Wang R, Reddy PH (2017) Role of glutamate and NMDA receptors in Alzheimer's disease. J Alzheimers Dis 57:1041–1048.

Wang X, Blanchard J, Grundke-Iqbal I, Iqbal K (2015) Memantine attenuates Alzheimer's disease-like pathology and cognitive impairment. Plos One 10:e0145441.

Xia P, Chen HS, Zhang D, Lipton SA (2010) Memantine preferentially blocks extrasynaptic over synaptic NMDA receptor currents in hippocampal autapses. J Neurosci 30:11246–11250.

Zajaczkowski W, Quack G, Danysz W (1996) Infusion of (+) -MK-801 and memantine – contrasting effects on radial maze learning in rats with entorhinal cortex lesion. Eur J Pharmacol 296:239–246.